Journal of Alloys and Compounds 509 (2011) 3269–3273

Contents lists available at ScienceDirect

Journal of Alloys and Compounds

journal homepage: www.elsevier.com/locate/jallcom

Cooling rate effect on Young's modulus and hardness of a Zr-based metallic glass

Z.Y. Liu [a], Y. Yang [a], S. Guo [a], X.J. Liu [a], J. Lu [a], Y.H. Liu [b], C.T. Liu [a,*]

[a] Department of Mechanical Engineering, The Hong Kong Polytechnic University, Hung Hom, Kowloon, Hong Kong
[b] WPI Advanced Institute for Materials Research, Tohoku University, Sendai 980-8577, Japan

ARTICLE INFO

Article history:
Received 6 November 2010
Accepted 13 December 2010
Available online 22 December 2010

Keywords:
Metallic glass
Cooling rate
Young's modulus
Hardness

ABSTRACT

It is known that cooling rate can affect the atomic structure and thus may possibly affect the mechanical properties of metallic glasses (MGs). In spite of the considerable efforts on the cooling rate, its effect on the mechanical properties is controversial at the present time. In this study, we present a micromechanical study of the cooling-rate effect on Young's moduli and hardness of the cast bulks and melt-spun ribbons for a $Zr_{55}Pd_{10}Cu_{20}Ni_5Al_{10}$ metallic glass. Using the classic nanoindentation method, the Young's moduli of the ribbon samples obtained at higher cooling rates were measured which appeared to be much lower than those of the bulk samples. However, through further experiments on slice samples cut from the as-cast bulks and finite-element (FE) analyses, we have clearly demonstrated that the measured difference in elastic moduli was mainly caused by the sample thickness effect in nanoindentation tests. To overcome such a confounding effect, microcompression experiments were performed on the as-cast and as-spun MG samples, respectively. Being consistent with the findings from nanoindentation, the microcompression results showed that the cooling rate, as ranging from $\sim 10^2$ to $\sim 10^6$ K/s, essentially has no influence on the Young's modulus and hardness of the metallic glasses.

1. Introduction

Metallic glasses (MGs), as a relatively new class of metallic materials, have received considerable attention due to their unique physical and mechanical properties [1–5]. Lacking long-range periodicity, MGs can be considered as solids with frozen-in liquid structures, which are composed of tightly bonded atomic clusters and free-volume zones [6]. Being in a metastable state, the glassy structure of MGs is most likely to be affected by different variables arising in the stage of materials preparation, for example, cooling rate, overheat temperature, and impurities [7–9], among which the cooling rate was thought to play an important role in the vitrification of MGs [10–12]. In that case, it was argued that the mechanical properties of MGs could also be affected by the cooling rate [11,13]. The increase of the cooling rate may result in configurationally looser atomic packing and thus, more free-volume zones [14,15], which therefore contributes to larger plasticity [16–18]. However, the cooling-rate effect on the yield strength of MGs is yet to be conclusive [16,19,20]; meanwhile, the studies concerning the cooling rate effect on the elastic behavior of MGs are limited. In view of these, further research effort is thus necessary for clarifying the aforementioned cooling rate effect.

Through a nanoindentation study, Jiang et al. [21] recently reported that the as-cast bulk $Cu_{60}Zr_{30}Ti_{10}$ metallic glasses had higher Young's moduli and hardness than the ribbons of the same composition. They attributed this to the less amount of free-volume zones in the bulk samples than in the ribbon samples, therefore reaching the conclusion that a faster cooling rate favors more free-volume zones. However, it should be pointed out here that, in the original indentation method developed by Oliver and Pharr, the testing sample was assumed to have a semi-infinite geometry [22]. The neglecting of such an implicit assumption when testing samples of finite dimensions, such as thin ribbons, could result in a sample thickness effect in nanoindentation, which tends to underestimate the true material's Young's modulus [23,24]. Unfortunately, the sample-thickness effect was somehow ignored by Jiang and co-workers, which means that it is necessary to carry out additional experiments as to clarify the cooling rate effect. In this study, the research work involved was organized as follows. First, nanoindentation tests based on the Oliver & Pharr's approach were carried out to investigate the cooling rate effect on the Young's modulus and hardness of bulk and ribbon MGs; second, the same testing method was extended to the MG samples with the same thickness but obtained at different cooling rates; third, finite element analyses (FEA) was performed to mimic the nanoindentation

* Corresponding author. Tel.: +852 27666644; fax: +852 23654703.
E-mail address: mmct8tc@inet.polyu.edu.hk (C.T. Liu).

0925-8388/$ – see front matter © 2010 Elsevier B.V. All rights reserved.
doi:10.1016/j.jallcom.2010.12.095

tests and assess the thickness effect on the extracted mechanical properties; finally, microcompression was utilized to verify the cooling rate effect on the Young's modulus and yield strength of the MGs.

2. Experimental procedure and numerical simulation

A quinary alloy of nominal composition $Zr_{55}Pd_{10}Cu_{20}Ni_5Al_{10}$ (atomic percentage) was chosen for the investigation due to its excellent glass-forming ability [25]. The master alloy ingots were prepared by arc-melting a mixture of the constituent elements with purity better than 99.9% in a Ti-gettered high purified argon atmosphere. Each ingot was re-melted several times to ensure the homogeneity of chemical composition. The bulk samples with diameter of 5 mm (Bulk I) and 1.5 mm (Bulk II) were produced by arc-melting and suction casting the ingots into a copper mold. The ribbon samples were prepared by remelting the ingots in a quartz tube and ejecting through a nozzle onto a copper wheel rotating at velocities of 2000 r/min (Ribbon I) and 4000 r/min (Ribbon II). The resulting ribbons had the dimensions of 44 μm (thickness) × 1.1 mm (width) and 20 μm (thickness) × 1.3 mm (width) respectively. After that, the amorphous structures of these as-cast bulk and as-spun ribbon samples were confirmed by X-ray diffraction and differential scanning calorimetry (DSC).

To measure the mechanical properties of the MG samples, standard nanoindentation method based on the Oliver and Pharr's approach was used to measure the Young's modulus and hardness of the MGs [22]. Prior to the nanoindentation tests, the surfaces of the MG specimens were mechanically polished to a mirror finish using 0.3 μm diamond paste. The standard Berkovich nanoindentation tests were then carried out at a constant loading rate of 10 mN/s with a peak load of 50 mN on the Hysitron TriboScratch® Nano Indenter. To clarify the sample thickness effect, slice samples with different thicknesses, ranging from 20 to 1550 μm, were sectioned employing wire cutting from the center of a bulk MG sample with diameter of 5 mm and subsequently tested using the same nanoindentation approach. For each sample, at least seven nanoindentation tests were carried out to obtain reliable data.

Supplementary to the experiments, numerical simulations of the nanoindentation tests were performed using the commercial package Abaqus™. A conical rigid indenter with a semi included angle of 70.3° was used in the FE model. For brevity, some details of building the FE model, such as meshing and checking of the influence of boundary conditions, which are not relevant to this particular problem, are omitted here. Interested readers may be referred to Ref. [26]. For simplicity, a rod-shaped MG specimen instead of a ribbon MG specimen was constructed in the FE model. In doing so, the three-dimensional FE problem is simplified to an axisymmetric one. To mimic the real indentation experiments, the MG sample and the substrate epoxy resin were assumed as elastic-perfect-plastic solids, and the MG–epoxy interface was taken as cohesive throughout the whole simulation.

Apart from nanoindentation, microcompression tests were also performed on both bulk and ribbon MG samples. To evaluate the cooling rate effect, micropillars were fabricated on the surfaces of one bulk (diameter 5 mm) and one ribbon (thickness 20 μm) sample using a dual-beam scanning electron microscopy (SEM)/focused ion beam (FIB) system (Quanta 200 3D, FEI). Following the sequential ion-milling approach [27], a series of micropillars having respective top diameters and aspect ratios ranging from ~1 to ~4 μm and 2:1 to 5:1, were carved out on the surfaces of the bulk and ribbon samples and later tested using a 10 μm flat-end conical diamond indenter with load control.

3. Results and discussion

3.1. Mechanical properties measured from nanoindentation

According to Lin and Johnson [28], the cooling rate, R, of MGs can be estimated as $R = 10/t^2$, where t is the cooling thickness of a MG sample. Based on this equation, the cooling rates of Bulk I, Bulk II, Ribbon I, Ribbon II were estimated as 1.60×10^2, 1.78×10^3, 6.25×10^5 and 3.09×10^6 K/s, respectively. Thus, the difference in cooling rates is over four orders of magnitude.

Typical indentation load–depth curves of the $Zr_{55}Pd_{10}Cu_{20}Ni_5Al_{10}$ bulk and ribbon MG samples are presented in Fig. 1. It is apparent that the maximum indentation depth is dependent on the cooling thickness and, thus, the cooling rate used during sample preparation. With the increasing cooling rate, the maximum indentation depth increases, as consistent with the previously finding [21]. However, it is worth mentioning that, for the ribbon samples corresponding to different cooling rates, the difference in the maximum indentation depths is small. To minimize the effect from the epoxy resin (as shown in the set of Fig. 1), all the indents were made in the middle of the ribbon samples' cross sections. Note that the indent has a size of ~3 μm and the distance between two indents is at least 30 μm apart.

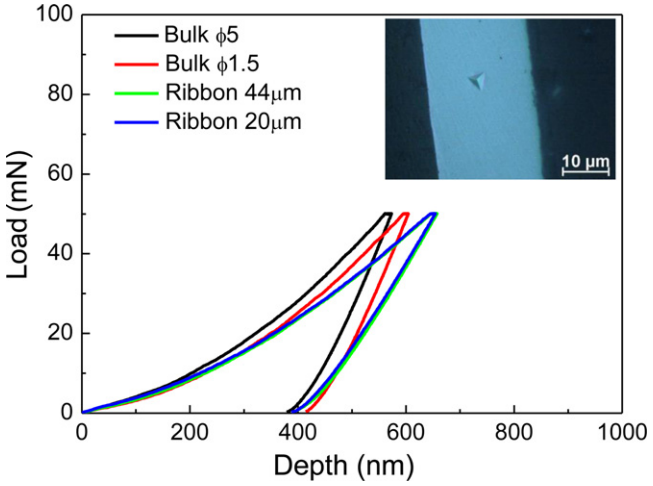

Fig. 1. Typical curves of load vs. depth for metallic glass samples with different cooling rate. Inset is the position of indent in the ribbon sample.

Following Oliver and Pharr [22], the Young's Moduli and hardness values were extracted from the nanoindentation load–depth curves and the results are listed in Table 1. Interestingly, the measured hardness values for all MG samples are about 5.3–5.5 GPa, essentially independent of the cooling rates. If the empirical relation between hardness and yield strength, $H \approx 3\sigma_y$ [29], was used, the estimated yield strength of the $Zr_{55}Pd_{10}Cu_{20}Ni_5Al_{10}$ MGs would be around ~1.8 GPa, which agrees quite well with the previous experimental results obtained from uniaxial compression tests [25]. The invariance of the hardness implies that the cooling rates, spanning four orders of magnitudes though, do not cause any apparent changes in the yield strengths of the MGs. In sharp contrast, the measured Young's moduli drop substantially from ~97 to ~64 GPa when the testing sample thickness reduces from 5000 μm to 20 μm, or the corresponding cooling rate increases from about $\sim 10^2$ to $\sim 10^6$ K/s. Note that this trend is consistent with the finding reported in Ref. [21]. In addition, through the thermodynamic parameters in Table 1 obtained from the DSC curves, it can be noted that the glass transition temperature (T_g) increases slightly with cooling rate, rising from 693 to 712 K when the cooling rate increases form about $\sim 10^2$ to $\sim 10^6$ K/s, while the crystallization temperature (T_x) is relatively stable around 776 K. The small change of the glass transition temperature indicates that the internal atomic structure has changed in certain degree, but this change is not sufficient enough to be revealed in the hardness data.

Since a material's Young's modulus, E, can be related to the material's inter-atomic potential and inter-atomic distance, we can have [30]:

$$E = V\left(\frac{d^2U}{dV^2}\right) = kr\frac{\partial}{\partial r}\left(\frac{1}{r^2}\frac{\partial U}{\partial r}\right) \quad (1)$$

Table 1
Young's moduli and hardness of the metallic glass samples with different cooling rate.

Samples	Thickness (μm)	T_g (K)	T_x (K)	E (GPa)	H (GPa)
Bulk I	5000	693	776	96.80 ± 0.81	5.26 ± 0.13
Bulk II	1500	696	775	94.01 ± 1.21	5.28 ± 0.09
Ribbon I	44	709	777	77.81 ± 1.53	5.51 ± 0.09
Ribbon II	20	712	776	63.67 ± 1.26	5.43 ± 0.21

Table 2
Young's moduli and hardness of the slice and bulk metallic glass samples with the same cooling rate.

	Slices cut from bulk Φ5			Bulk Φ5
	S1	S2	S3	Bulk I
Size (μm)	20	88	1550	5000
E (GPa)	63.42 ± 2.34	79.87 ± 2.90	94.30 ± 1.09	96.80 ± 0.81
H (GPa)	5.18 ± 0.05	5.51 ± 0.10	5.51 ± 0.11	5.26 ± 0.13

where V is the atomic volume, U is the inter-atomic potential, r is inter-atomic distance and k is a material constant. Normally, decreasing inter-atomic potential will lead to a lower elastic modulus given an unchanged inter-atomic distance. Since the tested MGs are of the same chemical composition, a similar shape in the inter-atomic potential is expected. Therefore, it is unlikely that the difference of four orders of magnitudes in the cooling rate, which only causes a density difference of less than 2% during materials preparation [14], can result in such a significant reduction in the Young's modulus.

To clarify whether other factors are responsible for the observed decrease in the Young's Modulus, three slices were cut from the center of a 5 mm bulk MG rod, which had the respective thickness of 20 μm (S1), 88 μm (S2) and 1550 μm (S3), and subsequently tested using the same nanoindentation approach. The measured Young's moduli and hardness of the slice samples are listed in Table 2. Interestingly, the measured Young's moduli from samples S1 and S2 are ~63 and ~80 GPa, respectively, much lower than that of the bulk sample from which the slices were cut. In contrast, the measured Young's modulus of Sample S3 slice is ~94 GPa, almost the same as that of the bulk sample. The experimental finding clearly demonstrates that varying sample thickness can greatly affect the material's Young's modulus measured from the nanoindentation. In comparison, the hardness measured from S1 to S3 shows no remarkable change with the varying sample thickness, which is consistent with the previous nanoidentation results obtained from the MG samples of different dimensions.

Fig. 2(a) presents the measured Young's moduli of the bulk, ribbon and slice MG samples. It is evident that the Young's moduli of the ribbon and slice samples are very close, exhibiting the same trend with the varying sample thickness. This experimental finding unambiguously proves that the seeming difference between the measured Young's moduli of the ribbon and bulk MG samples is mainly caused by the sample thickness instead of any physical change in the underlying atomic structures. In contrast, Fig. 2(b) shows the extracted hardness data of the bulk, ribbon and slice MG samples, which consistently display the trend of a constant value within the range of sample thickness from 20 μm to 5000 μm. This behavior can be understood as follows. From the mechanistic viewpoint, the Young's modulus reflects the rigidity of an elastically deformed volume and depends on the imposed boundary conditions, which becomes the 'source' of the sample thickness effect. However, hardness reflects the material's resistance to local plastic flows and is therefore less sensitive to the boundary conditions.

To verify the above arguments, FE simulations were carried out and the results are presented in Fig. 3 in comparison with the experimental data. Considering the difference of the sample geometry between the real and simulated MG samples and the uncertainties around the MG–epoxy interface, the simulation was motivated here only to check if the general trend of the experimental data could be captured. The procedure for 'calculating' the material's Young's modulus and hardness from simulation is as follows. First, the elastic-perfectly plastic MG FE model was assigned with a Young's modulus of 95 GPa and a yield strength of 2.2 GPa, and the epoxy in the vicinity of the MG model with the Young's modulus of 2 GPa and a yield strength of 0.04 GPa. Second, indentation was simulated by pushing the rigid conic indenter into the center of the MG

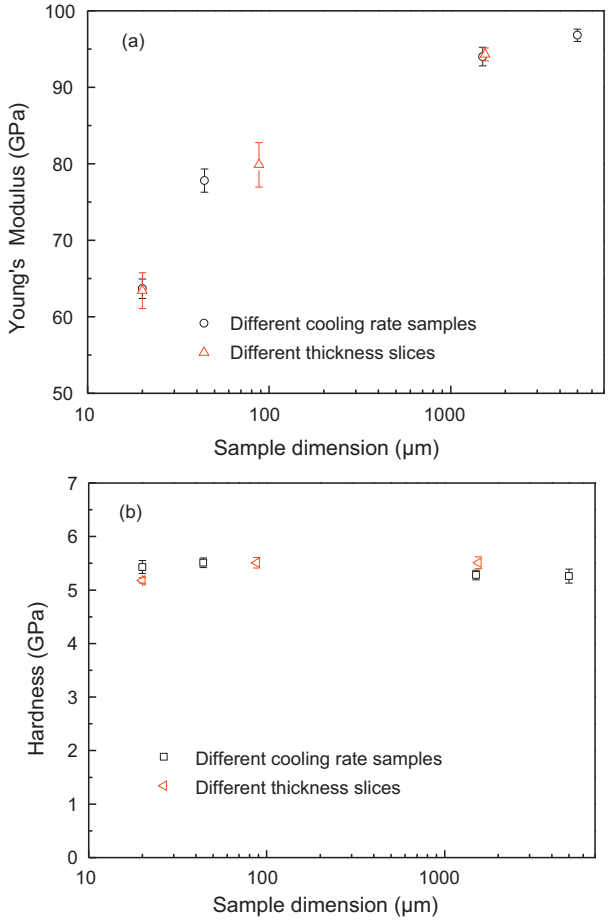

Fig. 2. (a) Young's modulus of bulk vs. ribbon (different cooling rate) and bulk vs. slice (different thickness) glassy samples. (b) Hardness of bulk vs. ribbon (different cooling rate) and bulk vs. slice (different thickness) glassy samples.

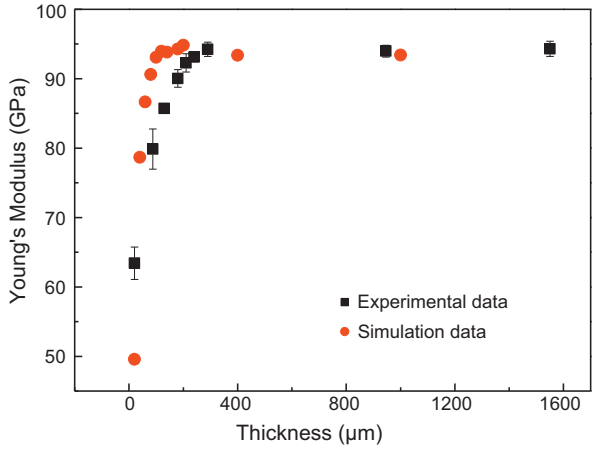

Fig. 3. Young's modulus dependence on sample thickness from experimental and simulation results.

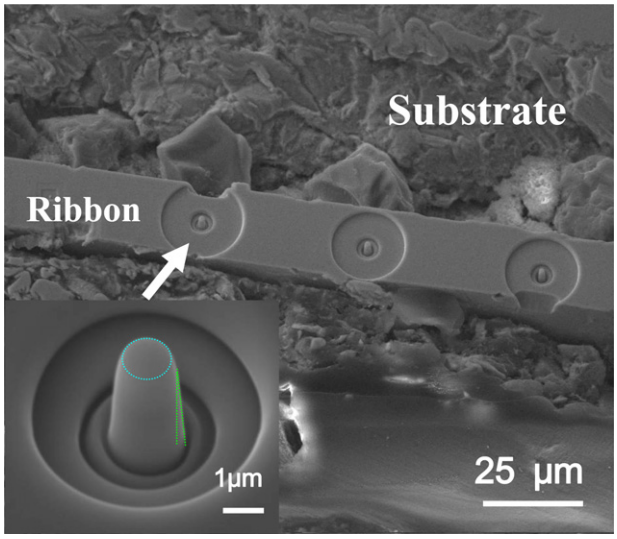

Fig. 4. Position of the fabricated micropillars in ribbon sample. Inset is the representative geometries of one micropillar.

model and, then, retracting the indenter backwards for unloading. After that, the Young's modulus and hardness were computed from the simulated load–displacement curves following the method proposed by Oliver and Pharr [22]. As shown in Fig. 3, the simulation results generally follows the trend of the experimental data in spite of the aforementioned model simplification, which, again, corroborate our previous conclusion that there should be no significant difference between the hardness and modulus of the MG bulk and ribbon samples.

3.2. Mechanical properties measured from microcompression

To exclude the confounding effect of sample thickness, microcompression tests were used to extract the mechanical properties of the bulk and ribbon MG samples. As shown in Fig. 4, a few micropillars were carved out on the surface of the 20 μm thick MG ribbon sample. Due to the ion-beam divergence, the micropillars were slightly tapered with an average taper angle of ~2°.

The microcompression experiments were subsequently conducted at a loading rate of 0.2 mN/s and the typical load–displacement curves are shown in Fig. 5, from which the Young's modulus and yield strength of a MG micropillar can be extracted. For micropillars with slight tapering, the Young's modulus, E, and yield strength, σ_y, can be obtained using the methods

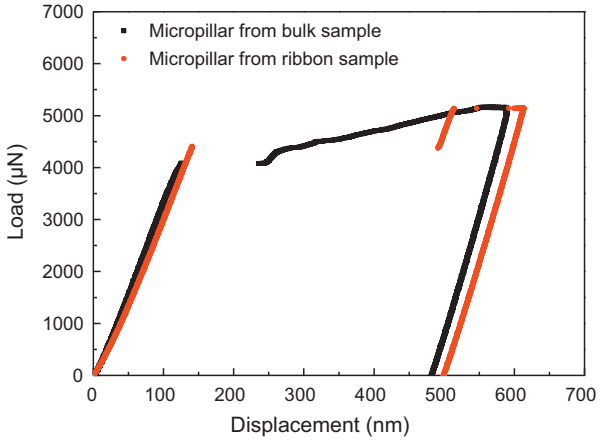

Fig. 5. Typical microcompression load–displacement curves of the micropillars.

Table 3
Young's moduli and yield strengths of the micropillars carved from bulk and ribbon samples with different cooling rates.

Micropillars	E (GPa)	σ_y (GPa)
From bulk sample	88.3 ± 5.66	2.2 ± 0.13
From ribbon sample	88.2 ± 2.60	2.3 ± 0.21

proposed in Refs. [27,31]. As listed in Table 3, it can be seen that the Young's moduli and yield strengths of the micropillars cut from the bulk and ribbon samples are almost the same, with the average value being ~88 GPa and 2.2 GPa, respectively. This further confirms that the cooling rate has a negligible effect on the Young's modulus of MG samples. Before proceeding, it is worth mentioning that the Young's modulus obtained from microcompression is about 5% lower than the values extracted from nanoindentation tests. This is because of the material's pile-up effect, which was not taken into account in the original Oliver and Pharr's method [22]. For MGs, the neglecting of such a pile-up effect will lead to an overestimation of the material's Young's modulus [32]. In addition, the yield strengths obtained from the microcompression tests appear to be higher than those from the conventional uniaxial compression tests [25], which is usually attributed to the Weibull statistics as already discussed in the literature [33].

3.3. Implications

Based on the above analyses and discussions, we have demonstrated that the cooling rate used in our study, ranging from ~10^2 to ~10^6 K/s, does not cause any remarkable change in the Young's modulus and hardness of the Zr-based MG samples, though small changes in the glass transition temperature have been detected. This is implicative of a similar atomic structure in the MGs in spite of the large cooling-rate difference. The reason might lie in two folds: (1) the cooling rates employed in the study were still below a critical value, only above which a sufficient structural change can be detected from the hardness and Young's modulus of MGs [14]; and (2) the overheat temperature, from which the molten metals were quenched, was not high enough for the atomic clusters and free-volume zones to rearrange [34]; in other words, the atomic structure of the metallic glass was mainly determined by the overheat temperature rather than the cooling rate imposed during quenching process.

4. Conclusions

Based on the current work, we find that the cooling rate has a negligible influence on the Young's modulus and hardness of the $Zr_{55}Pd_{10}Cu_{20}Ni_5Al_{10}$ metallic glass, which is contrary to the previous findings [21]. The apparent reduction in the Young's moduli of the ribbon samples relative to those of the bulk samples, as measured using nanoindentation, has been proved simply caused by sample thickness. After eliminating such a sample geometry effect, the cooling-rate independent mechanical properties were attained. Such an insignificant influence of the cooling rate on the Young's modulus and hardness of the Zr-based MG implies that a faster cooling rate is needed for further research or the overheat temperature is not high enough to introduce any significant physical change in the glassy structure of the Zr-based MGs.

Acknowledgements

This research was supported by an internal funding from HKPU. In addition, Y.Y. acknowledges the financial support provided by the Hong Kong Polytechnic University for newly recruited academic staff (Project code: G-YH85).

References

[1] M.W. Chen, Annual Review of Materials Research 38 (2008) 445–469.
[2] A.L. Greer, E. Ma, MRS Bulletin 32 (2007) 611–615.
[3] C.A. Schuh, T.C. Hufnagel, U. Ramamurty, Acta Materialia 55 (2007) 4067–4109.
[4] A.R. Yavari, J.J. Lewandowski, J. Eckert, MRS Bulletin 32 (2007) 635–638.
[5] J.F. Loffler, Intermetallics 11 (2003) 529–540.
[6] C. Fan, P.K. Liaw, C.T. Liu, Intermetallics 17 (2009) 86–87.
[7] Y.Q. Cheng, A.J. Cao, H.W. Sheng, E. Ma, Acta Materialia 56 (2008) 5263–5275.
[8] G. Kumar, T. Ohkubo, K. Hono, Journal of Materials Research 24 (2009) 2353–2360.
[9] C.T. Liu, M.F. Chisholm, M.K. Miller, Intermetallics 10 (2002) 1105–1112.
[10] J.T. Wang, P.D. Hodgson, J.D. Zhang, W.Y. Yan, C.H. Yang, Journal of Materials Processing Technology 209 (2009) 4601–4606.
[11] D.V. Louzguine-Luzgin, T. Saito, J. Saida, A. Inoue, Journal of Materials Research 23 (2008) 515–522.
[12] L.Q. Xing, T.C. Hufnagel, J. Eckert, W. Loser, L. Schultz, Applied Physics Letters 77 (2000) 1970–1972.
[13] Y. Liu, H. Bei, C.T. Liu, E.P. George, Applied Physics Letters 90 (2007) 071909.
[14] X. Hu, S.C. Ng, Y.P. Feng, Y. Li, Physical Review B 64 (2001) 172201.
[15] A. Rehmet, K. Gunther-Schade, K. Ratzke, U. Geyer, F. Faupel, Physica Status Solidi A 201 (2004) 467–470.
[16] L.Y. Chen, A.D. Setyawan, H. Kato, A. Inoue, G.Q. Zhang, J. Saida, X.D. Wang, Q.P. Cao, J.Z. Jiang, Scripta Materialia 59 (2008) 75–78.
[17] Y.H. Xiao, Y. Wu, Z.Y. Liu, H.H. Wu, Z.P. Lu, Science China-Physics Mechanics & Astronomy 53 (2010) 394–398.
[18] J. Shen, Y.J. Huang, J.F. Sun, Journal of Materials Research 22 (2007) 3067–3074.
[19] Y.J. Huang, J. Shen, J.F. Sun, Applied Physics Letters 90 (2007) 081919.
[20] J. Zhang, S.J. Pang, T. Zhang, Science China-Physics Mechanics & Astronomy 53 (2010) 415–418.
[21] W.H. Jiang, F.X. Liu, Y.D. Wang, H.F. Zhang, H. Choo, P.K. Liaw, Materials Science and Engineering A 430 (2006) 350–354.
[22] W.C. Oliver, G.M. Pharr, Journal of Materials Research 7 (1992) 1564–1583.
[23] J.M. Antunes, J.V. Fernandes, N.A. Sakharova, M.C. Oliveira, L.F. Menezes, International Journal of Solids and Structures 44 (2007) 8313–8334.
[24] F.Q. Yang, Materials Science and Engineering A 358 (2003) 226–232.
[25] Y.H. Liu, C.T. Liu, A. Gali, A. Inoue, M.W. Chen, Intermetallics 18 (2010) 1455–1464.
[26] N.A. Sakharova, J. Fernandes, J.M. Antunes, M.C. Oliveira, International Journal of Solids and Structures 46 (2009) 1095–1104.
[27] Y. Yang, J.C. Ye, J. Lu, F.X. Liu, P.K. Liaw, Acta Materialia 57 (2009) 1613–1623.
[28] X.H. Lin, W.L. Johnson, Journal of Applied Physics 78 (1995) 6514–6519.
[29] L.A. Davis, Mechanical Behavior of Rapidly Solidified Materials, The Metallurgical Society, Pittsburgh, 1986.
[30] F. Zeng, Y. Gao, L. Li, D.M. Li, F. Pan, Journal of Alloys and Compounds 389 (2005) 75–79.
[31] J.C. Ye, J. Lu, Y. Yang, P.K. Liaw, Intermetallics 18 (2009) 385–393.
[32] Y. Choi, H.S. Lee, D. Kwon, Journal of Materials Research 19 (2004) 3307–3315.
[33] W.F. Wu, Z. Han, Y. Li, Applied Physics Letters 93 (2008) 061908.
[34] C. Fan, D. Chen, P.K. Liaw, H. Choo, C. Benmore, J. Siewenie, G.L. Chen, J.X. Xie, C.T. Liu, Applied Physics Letters 93 (2008) 261905.